Cryogenic and Low-Temperature Heat Pipe/Cooler Studies for Spacecraft Application

A. Sherman*
NASA Goddard Space Flight Center, Greenbelt, Md.
and
P. Brennan†
B & K Engineering, Inc., Towson, Md.

Several important conclusions can be drawn from an analysis of an 80-100°K radiant cooler/heat pipe system for NASA spacecraft applications. Within reasonable temperature excursions, working fluid property variations have little effect on system performance. This allows the system to operate over a range of cooling loads with the cooler temperature controlled by a heater. The system size and weight are strongly dependent upon heat pipe length and diameter because of the parasitic load effect. Present day NASA coolers could not accomodate a practical heat pipe because of this effect, and larger heat pipe cooler systems would be required in the 80-100K range. An optimized heat pipe for this system is one whose diameter is as small as practical, but consistent with the transport and priming requirements imposed by ground testing and the zero-g application. The composite slab wick configuration appears to offer a reliable, "state-of-the-art" heat pipe with adequate capacity to meet both present day and projected NASA radiant cooler applications. Heat pipe diameters on the order of 1.0 cm have theoretical transport capabilities greater than 2.5 W-m in the 80-100K temperature range with conventional composite slab wicks and nitrogen or oxygen working fluids. An analysis of a solid cryogen/heat pipe/radiant cooler system indicates that for special applications this system provides a weight savings when compared to a two stage solid cryogenic cooler.

Nomenclature

A_e = effective heat transfer area of secondary cryogen shroud
A_p = radiant cooler patch area
A_p^* = radiant cooler patch size for reference-point cooler
A_{HT} = heat pipe parasitic load heat transfer area = $\pi D_{HP} L_{HP}$
A_v = vapor flow area
A_w = wick cross-sectional area
D = diameter
D_H = hydraulic diameter of vapor flow
g_0 = gravitational constant
h = heat pipe elevation
H_S = static elevation head
h_s = heat of sublimation of primary solid cryogen
h_s^* = heat of sublimation of secondary solid cryogen
k = heat pipe permeability
K_1 = radiation heat transfer coefficient from the first stage of the cooler to the patch
K_2 = conduction heat transfer coefficient from the first stage to the patch for a radiant cooler
K_3 = thermal conductance of cooler patch mount
K_1^* = K_1 for a reference-point cooler
K_2^* = K_2 for a reference-point cooler
$K(T_p)$ = heat pipe effect conductance
$K'(T_p)$ = $d[K(T_p)]/dT_p$
ℓ = length of cylindrical primary cryogen
L = length
M^* = mass of secondary solid cryogen
N = transport factor
Q_A = albedo heat input
Q_{COND} = conduction load from first stage of radiant cooler to the patch
Q_E = earth heat input
Q_{HP} = heat pipe parasitic load
Q_L = cooling load (e.g. detector heat dissipation)
Q_{OP} = optical port load
Q_{RAD} = radiation load from first stage of radiant cooler to the patch
(QL_{eff}) = heat pipe transport capability
$(QL)_{REQD}$ = heat pipe transport requirement
Q_S = solar heat input
r_p = effective pumping radius
r_f = radius of cylindrical primary cryogen
T_E = ambient temperature (294 K)
T_{HP} = average temperature of heat pipe
T_L = cooling load (e.g. detector) temperature
T_M = mission time
T_1 = temperature of solid cryogen cooler inner shell temperature
T_p = radiant cooler patch temperature
T_{r1} = radiant cooler first stage temperature
γ = wicking height factor
$\bar{\epsilon}$ = effective emissivity of multi-layer insulation of solid cryogen cooler
$\bar{\epsilon}_H$ = effective emissivity of multi-layer insulation around a heat pipe
ϵ_p = radiator patch emissivity
η = gravity factor
ν = kinematic viscosity
ρ = density
σ = Boltzmann's Constant
σ_ℓ = liquid surface tension

Subscripts

c = condenser
e = evaporator
HP = heat pipe
ℓ = heat pipe liquid
v = heat pipe vapor
s = primary cryogen

Presented as AIAA Paper 74-753 at the AIAA/ASME 1974 Thermophysics and Heat Transfer Conference, Boston, Massachusetts, July 15-17, 1974; received July 23, 1975. The paper's title refers to spacecraft temperature control systems.

Index category: Spacecraft Temperature Control Systems.

*Aerospace Technologist, Thermal Systems Branch, Systems Division.

†Manager.

Introduction

POTENTIAL applications for cryogenic or low-temperature heat pipes aboard spacecraft include 1) the coupling of one or several detectors to individual or multiple passive and/or active coolers,[1] 2) isothermalization of radiant coolers,[1] 3) coupling of optical packages to coolers, and 4) hybrid cooler systems (e.g. Fig. 1). Cryogenic heat pipes might also find application as interface components between radiators and large multiple detector arrays, or to provide for detachable detectors and/or radiators for shuttle resupply. The use of cryogenic diode heat pipes has also been considered for applications in which the cooler is exposed to a hot environment such as cyclic solar or earth inputs. When the cooler becomes warmer than the heat source (e.g. detector or optical compartment), the diode pipe shuts down to isolate the system from the hot environment.

A review of the literature shows an increasing amount of work on low temperature heat pipes. Brennan et al.[2] obtained 77 K data for nitrogen heat pipes with axial grooved and arterial wick configurations, while Wright et al.[1] report on the development of a low-temperature heat pipe/radiator and heat pipe transport system for detector cooling. The axial groove wick geometry is employed in the latter reference. Freon-14 is used in the radiator pipes (130 K), and methane is employed in the transportors (130-150 K). Murray[3] shows test data for 2-W methane heat pipes at 110 K which employ a wire cloth wick. Extensive performance data for an extruded axial groove geometry charged with oxygen, methane and ethane and operated in the 100-200 K range is presented in Ref. 4.

The prime purpose of the present work is to examine cryogenic heat pipe/cooler feasibility in the 80-100 K temperature range and in the regimes of operation required for NASA spacecraft. Present requirements within these regions are 1) cooling load of less than 1-2 W per cooler, 2) small detector/heat pipe interface area, and 3) high systems reliability and long lifetime operations.

The cooling capacity of practical radiant coolers is very low in this temperature range and very temperature sensitive. Detector performance is also strongly dependent on temperatures in this regime. It is, therefore, important to understand the interplay of the heat pipe and its effects on overall system performance. As will be developed, the heat pipes' size and thermal conductance directly impact the cooler design. Finally, a change in heat load could alter the radiant cooler temperature and thereby change the heat pipes' operating characteristics. Since candidate cryogenic fluids for the range of interest can experience substantial property variations for relatively small changes in temperature, it is imperative that their effect on heat pipe and system performance be known and predictable.

As the systems part of this study developed it became clear that an evaluation of past and potential cryogenic heat pipe types was required. This was done by analysis, data review, and some new testing. Emphasis on this evaluation was put on nitrogen heat pipes, although oxygen pipes were considered. Hopefully, the results of this evaluation, together with the systems studies, will point the way towards the types of heat pipes which are practical for these low-temperature range applications.

Finally, in an effort to identify possible new low-temperature heat pipe/cooler systems, a brief analysis is presented to indicate the feasibility of a hybrid solid cryogen/passive cooler system which employs a low-temperature heat pipe.

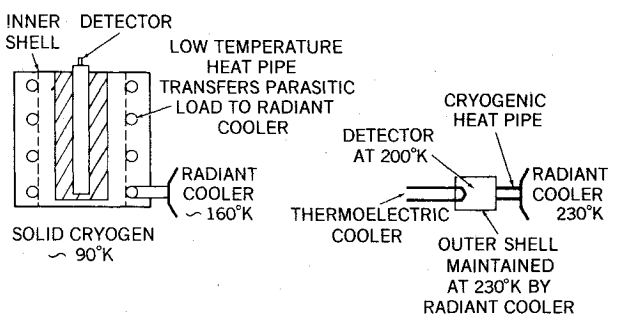

Fig. 1 Hybrid coolers employing heat pipes.

Radiant Cooler/Heat Pipe System

General Configuration

Figure 2 shows a general schematic of a low-temperature or cryogenic heat pipe/radiant cooler system. Typically the cooler is constructed in two stages. The first stage consists of a cone with a highly reflective inner surface and a radiator which cools the cone to 170 K. The purpose of the cone is to shield the primary radiator (patch) from the spacecraft and Earth, or to reflect shallow-angle sun input out of the cooler before it reaches the patch. Further isolation from the spacecraft is obtained by mounting the patch to the first stage with low-conductive supports. If shielding from the spacecraft is not required, and there is no sun input to the cooler, the second-stage cone can be eliminated and a deployable door attached to the mouth of the first stage can be used to block the patch's view of the earth.

For coolers presently in operation, the components requiring cooling (e.g. detector) are mounted directly to the patch. The addition of a cryogenic heat pipe into the system, while allowing greater flexibility in spacecraft and instrument design, introduces new problems and limitations which must be considered.

The parasitic load impressed upon a cryogenic heat pipe aboard an ambient temperature spacecraft is

$$Q_{HP} \simeq \sigma \bar{\epsilon}_H \pi (DL)_{HP} (T_E^4 - T_{HP}^4) \quad (1)$$

The heat rejection capacity of a patch on present-day NASA radiator coolers is approximately 30-MW. For a heat pipe length of 1 m, and good multi-layer insulation ($\bar{\epsilon}_H \simeq 0.01$), the parasitic load from a 3-mm diam heat pipe would alone exceed present-day cooler capacity.

The effect of heat pipe size and parasitic load on required patch area is estimated in the following analysis for a cooler without a cone. An energy balance for the patch, neglecting Earth, albedo, and solar input yields

$$\sigma \epsilon_p T_p^4 = Q_{OP} + Q_{COND} + Q_{RAD} + Q_{HP} + Q_L \quad (2)$$

where

$$Q_{RAD} = K_1 (T_{r1}^4 - T_p^4) \quad (3)$$

$$Q_{COND} = K_2 (T_{r1} - T_p) \quad (4)$$

Now, taking present day NASA coolers as a reference point we assume that

$$K_1 \simeq K^* (A_p / A_p^*) \quad (5)$$

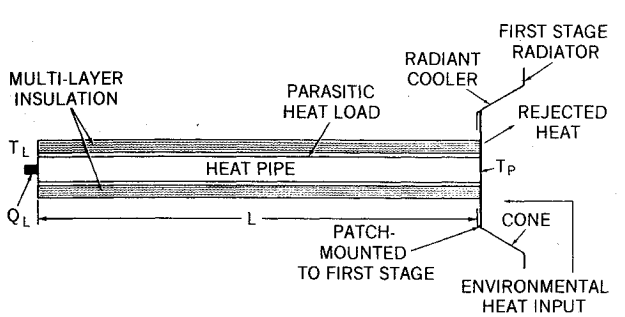

Fig. 2 Schematic of radiant cooler/heat pipe system.

$$K_2 \simeq K^*(A_p/A_p^*) \tag{6}$$

Combining Eqs. (1)-(6)

$$A_p = \frac{Q_L + Q_{OP} + \sigma\pi(\bar{\epsilon}_H D_{HP} L_{HP})(T_E^4 - T_p^4)}{-K_1^*/A_p^*(T_{r1} - T_p) - K_2^*/A_p^*(T_{r1} - T_p) + \sigma\epsilon_p T_p^4} \tag{7}$$

The plot of Eq. (7) is shown in Fig. 3. The reference-point constants were taken at their values for a typical present day NASA cooler. Also, the figure shows two cases (dotted lines) which represent the extreme values of $\bar{\epsilon}_H D_{HP}$ which are of interest here.

Figure 3 can be used to estimate the radiant cooler patch area required for a heat pipe/cooler system with a given optical and detector load. For example, for a present day cooler with a fixed load of about 20 mW the curves show that a 50 cm^2 patch is required. If a 1 m long, 6.3 mm o.d. heat pipe with $\bar{\epsilon}_H = 0.01$ is included in the system, the patch area increases to 240 cm^2.

This analysis illustrates that because of the inherent parasitic loads, a cryogenic heat pipe/radiative cooler combination must be considered as a system, rather than as an addition of a cryogenic heat pipe to an existing radiator. Also, larger radiant coolers than are presently being developed are required to accommodate both the heat pipe and the larger cooling loads of future applications. Finally, it should be noted that as the cooler temperature level increases, the effect of the heat pipe on system performance becomes less significant because its parasitic losses decrease whereas the cooler capacity increases.

Cooler Sensitivity

The thermal conductivities of cryogenic fluids generally decrease with temperature. Therefore, a higher-than-expected cooling load would result in an increase in load temperature due to both a higher heat pipe temperature drop and an increase in radiant cooler temperature. An analysis was performed to predict the sensitivity of heat source temperature to changes in cooler load [i.e., (dT_L/dQ_L)]. Details of the analysis are presented in Ref. 6. For typical coolers, the major effect on the heat source temperature T_L is caused by an increase in patch temperature with increasing heat load. The effect of the decrease in conductivity which tends to further increase heat pipe operating temperature is relatively small and tends to be cancelled out by the corresponding decrease in parasitic losses.

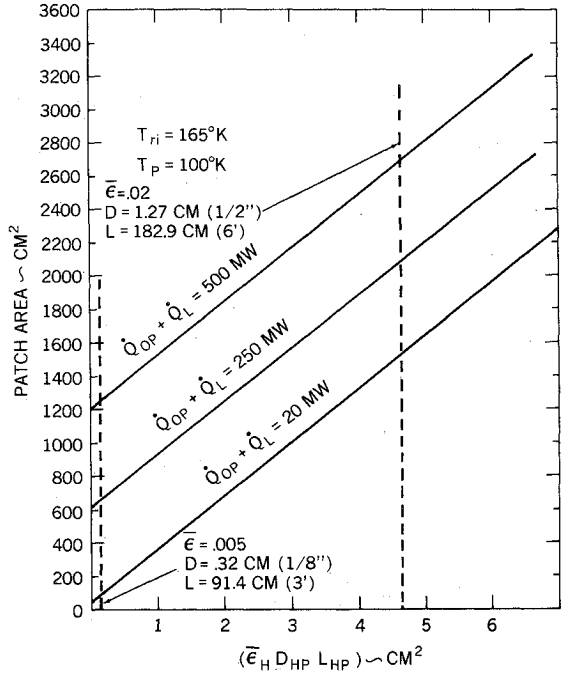

Fig. 3 Radiant cooler patch area vs $\bar{\epsilon}_H D_{HP} L_{HP}$.

Heat Pipe Requirements

It is obvious from the previous system's analysis that a heat pipe/radiator cooler will be optimized by using as small a diameter heat pipe as possible. In these applications, heat pipe diameters should be minimized within practical fabrication limits and the following design criteria: 1) satisfy thermal conductance (ΔT) requirements; 2) satisfy "0-g" transport requirements; 3) permit meaningful "1-g" testing.

The heat loads and consequently the temperature drops experienced in these applications are minimal. For those instances where the heat flux may be too high, the diameter of the heat pipe can be enlarged in the evaporator and/or condenser section to accomodate the ΔT requirements. The last two criteria relate to the transport capability of the heat pipe. In this regard, because of the rather small heat loads, vapor limits such as sonic vapor and entrainment do not apply, and the transport capability of the heat pipe is determined by the conventional capillary pumping limit.[7]

In order to establish whether a particular heat pipe's transport capability is adequate, one must first determine the transport requirements associated with the application. For the simple case of a single evaporator and condenser at opposite ends of the pipe with a parasitic load applied over the length of the pipe

$$(QL)_{REQD} = (Q_{OPT} + Q_{HP})(\tfrac{1}{2}L_e) + [Q_{OPT}L_T + Q_{HP}(\tfrac{1}{2}L_t)] + (Q_{OPT} + Q_{HP})(\tfrac{1}{2}L_c) \tag{8}$$

where

$$Q_{OPT} = Q_{OP} + Q_L$$

In many of these applications the evaporator and condenser lengths will be small compared to the total length and therefore a conservative approximation of the transport requirement is

$$(QL)_{REQD} \simeq [Q_{OPT} + \tfrac{1}{2}Q_{HP}]L_{HP} \tag{9}$$

It is interesting to note that in this case, because of the effect of the parasitic heat load, the transport requirement becomes a function of L_{HP}^2, vs the linear dependence commonly experienced when parasitic losses are negligible.

The transport requirement is presented in Fig. 4 vs heat pipe length with Q_{OPT} and $(\bar{\epsilon}D_{HP})$ as parameters. If a 2-m long × 1.27-cm o.d. heat pipe were employed in present NASA applications ($Q_{OPT} \simeq 25$ mW) it would have to accommodate a transport requirement of approximately 0.55 W-m. The

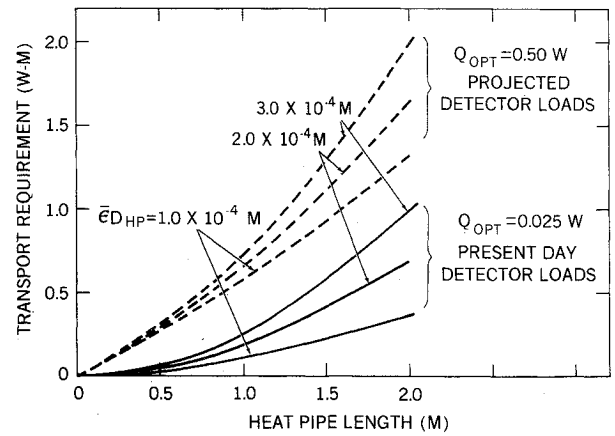

Fig. 4 Transport requirements for a heat pipe/radiant cooler system.

transport requirement for the same pipe with a projected detector load of 0.5 w would increase to 1.5 W-m.

These transport requirements are relatively low for cryogenic fluids. The 1.27-cm o.d. axial groove and arterial heat pipes tested in Ref. 2 both have measured transport capabilities with nitrogen at 80 K in excess of 15 W-m. The capacity with oxygen could be almost twice as high. Although these pipes have high transport capability, they do have inherent problems. Present day arterial pipes still have not demonstrated reliable start-up. The existing axial groove geometry has very low static heights with oxygen and nitrogen, and puddling effects obscure the "1-g" test data.[5] Homogeneous and composite slab wicks[8] have proven reliability and are potential alternatives to the artery and axial groove provided that they have adequate transport capability.

As regards the choice of working fluids, in addition to nitrogen and oxygen other candidates for the 80-100 K range are fluorine, carbon monoxide, argon, and methane. However, flourine and carbon monoxide present serious safety problems, argon has too narrow an operating temperature range and methane's freezing point is 88.7 K. Methane also experiences high vapor losses and start-up problems up to approximately 100 K. As a result, nitrogen and oxygen represent the best choice and are the only fluids considered in the subsequent analysis.

Cross sections of horizontal, homogeneous and composite slab wick designs are presented in Fig. 5. The analysis neglects fillet flow and assumes that the secondary wick does not affect the transport capability of the system. With these assumptions, the transport capability (QL_{eff}) for a slab heat pipe with uniform flow areas and wick properties is given by[6]

$$(QL_{eff}) = \frac{2kA_w}{r_p} F_\ell N_\ell (1+\eta) \tag{10}$$

where "perfect wetting" has been assumed and

$$F_\ell = \left[1 + \frac{\nu_v}{\nu_\ell} \frac{32k}{D_H^2} \frac{A_w}{A_v}\right]^{-1} \tag{11}$$

and for a horizontal slab geometry

$$\eta = -\frac{r_p D_{HP}}{4\gamma} + \frac{r_p h}{2\gamma} \tag{12}$$

with

$$\gamma = \frac{\sigma_\ell}{\rho_\ell g_0} \tag{13}$$

In order to provide reliable and easily interpreted l-g test results, as well as accomodate projected requirements the horizontal slab geometry should satisfy the following criteria: 1) static height $H_s \geq$ 1.0-cm + $D_{HP}/2$; 2) transport capability ~3.0 W-m@0.2-cm heat pipe elevation (factor of two design margin; 3) the composite slab should self-prime at elevations $\geq$0.2-cm + $D_{HP}/2$.

The first criterion is applied to guarantee that the wick will not begin to drain at very shallow elevations and result in puddling effects. This criterion is satisfied if

$$r_p \leq \frac{2\gamma}{H_s} \tag{14}$$

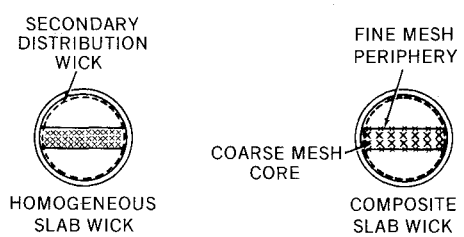

Fig. 5 Homogeneous and composite slab wick designs.

For a 0.635-cm o.d. oxygen pipe a 60 mesh screen size is required. Finer mesh sizes are needed to accommodate larger diameters and/or nitrogen. A calculation of the transport capability based on this first constraint indicates that at best a 1.27-cm o.d. homogenous slab with oxygen provides marginal transport (i.e., 3.0 W-m) over the temperature range. A nitrogen heat pipe, because of the lower liquid transport factor and the finer screen required, has less than half the capability of an oxygen pipe.

The poor performance of the homogeneous wick is caused by the low permeability or, more appropriately, the low ratio of k/r_p associated with the fine mesh size needed to satisfy the static height requirement. With a composite slab, the outer layer is a fine mesh screen that provides the capillary pumping, whereas the inner core is a more permeable heavier mesh whose pore size is determined by the less stringent self-priming criterion. As a result, composites can provide capacities substantially larger than that afforded by the homogeneous configurations. Figure 6 shows the optimum transport capabilities of 1.27 and 1.0-cm o.d. pipes with oxygen and nitrogen over the applicable temperature range.

The optimization is based on using a wick area which maximizes the transport capability. The permeability of the coarse wick is consistent with the mesh size required to satisfy the self-priming criterion (i.e., #3 above), and 200-mesh screen is used for pumping. The 200-mesh was selected because it satisfies the static height requirement for both fluids over the temperature range. It is also approximately the finest mesh size that can be used without having the secondary wick become the limiting factor.

The results indicate that oxygen can satisfy the projected transport requirement with either diameter heat pipe. The maximum performance for the 1.27-cm o.d. oxygen pipe is approximately 30 W-m at 80 K, which decreases to 14 W-m at 100 K. Higher vapor losses as well as the reduced wick area result in a maximum QL_{eff} of 5 W-m for the 1.0-cm pipe with oxygen. The maximum is reached at 95 K where the vapor losses are less dominant.

Nitrogen has a liquid transport factor which is about half that of oxygen's over the temperature range. In addition its wicking factor (γ) is lower and it therefore requires a finer mesh core to satisfy self-priming. This combination results in the lower transport capability. At 80K, QL_{eff} is approximately 8 W-m and this decreases to less than 2 W-m at 100 K with the 1.27-cm o.d. The capacity with the smaller diameter is less than 3 W-m over the entire range. The reduction in capability between the two diameters is less pronounced for nitrogen because it experiences lower vapor losses than oxygen at these temperatures.

A single data point obtained with a comparable 200-50 mesh composite slab with nitrogen in a 1.27-cm o.d. heat pipe is indicated in Fig. 6. This pipe had the wick oriented vertically and demonstrated a capability of about 4 W-m in l-g-tests. Although this is only half of the optimized prediction, it

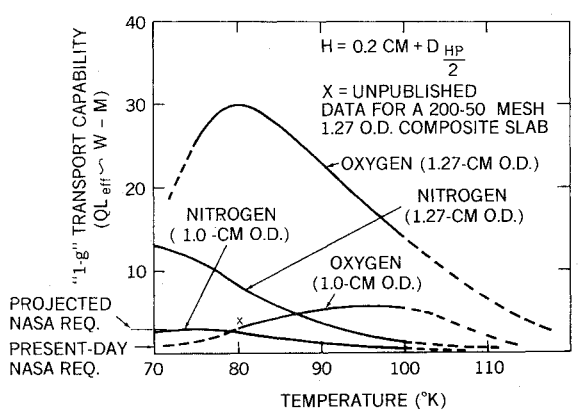

Fig. 6 "l-g" transport capability vs temperature.

does indicate the potential of the basic composite slab. A larger wick in the test pipe would have resulted in higher performance.

Solid Cryogen/Radiant Cooler System

Figure 7 shows schematic diagrams of both the two stage solid cryogen and a hybrid system employing a cryogenic heat pipe. The two stage cooler consists of a primary cryogen (e.g., methane at 90 K) and a secondary cryogen (e.g., ammonia at 160 K) which vent to space. The vent is designed such that the cryogen pressures are always below their triple points. Thus the cooling process is one of sublimination of the solid cryogen while maintaining the load at a constant temperature. The secondary cryogen maintains an isothermal shroud around the primary cryogen and thus absorbs the net external loads to the shroud. The primary cryogen then absorbs all radiative loads from the shroud, the detector assembly, and the conductive load from the secondary cryogen container to which it is mounted. The secondary cryogen must have a higher heat of sublimination than the primary in order for it to offer a weight advantage over a single stage system. Nevertheless, the weight of the secondary cryogen and assembly can be substantial for long duration flights.

A solid cryogen/heat pipe/radiant cooler system as depicted in Fig. 8 might be an alternative to the two stage cooler. A device of this nature could be used aboard a spacecraft where the environment precludes the use of a low temperature radiator ($\simeq 100$ K), but would be compatible with a moderate temperature radiator ($\simeq 160$ K). In this system, the low-temperature heat pipe and radiator replace the secondary cryogen. The shroud maintains its temperature by transferring its head load through the heat pipe to the radiator. The heat pipe could be wrapped around the shroud as shown in Fig. 8, or it could interface at a single location. This would depend upon the particular system design and the heat fluxes. In this application, a low-temperature heat pipe with possibly ethane as the working fluid[5] would be used. This type of system offers potentially longer life and/or higher load capacities without a prohibitive weight. The following analysis was performed to indicate potential weight savings of the hybrid system compared to a two stage solid cryogen cooler.

First, an equation for estimating the weight of the secondary solid cryogen on a two stage system will be developed. For a cylindrically shaped primary solid cryogen of radius r and length ℓ

$$\frac{A_e}{M} \simeq \frac{2\pi(r\ell+r^2)}{\rho_s \pi r^2 \ell} = \frac{1}{\rho_s}\left[\frac{2}{r}+\frac{2}{\ell}\right] \tag{15}$$

Now, assuming $2r=\ell$, and neglecting all but radiative heat transfer losses, a heat balance on the primary cryogen yields

$$\bar{\epsilon}\frac{3}{\rho_s r}\sigma(T_1^4-T_s^4) = \frac{h_s}{T_M} \tag{16}$$

or

$$r = \frac{3T_M}{\rho_s h_s}\bar{\epsilon}\sigma(T_1^4-T_s^4) \tag{17}$$

Hence

$$A_e \simeq 6\pi r^2 = 54\pi\left\{\frac{T_M\bar{\epsilon}}{\rho_s h_s}\sigma(T_1^4-T_s^4)\right\}^2 \tag{18}$$

Again only considering radiant heat transfer for the secondary cryogen

$$\sigma\bar{\epsilon}A_e(T_E^4-T_1^4) \simeq \frac{h_s^* M^*}{T_M} \tag{19}$$

Combining Eqs. (18) and (19) and rearranging

$$\frac{M^*}{\frac{T_M}{h_s}54\pi(\sigma\bar{\epsilon})^3\left[\frac{T_M}{\rho_s h_s}\right]^2 T_E^4 T_s^8} = \left[\left[\frac{T_1}{T_s}\right]^8 - 2\frac{T_1}{T_s}+1\right]\left[1-\left[\frac{T_1}{T_E}\right]^4\right] \tag{20}$$

For the hybrid system, a heat balance on the solid cryogen and radiator yields

$$\bar{\epsilon}A_c\sigma(T_1^4-T_s^4) = \frac{M}{T_M h_s} \tag{21}$$

and

$$\bar{\epsilon}A_e\sigma(T_E^4-T_1^4)+K_3(T_E-T_1) \simeq \sigma\epsilon_p A_p T_1^4 \tag{22}$$

where we are again only considering radiant heat transfer to the primary cryogen, and the conduction and heat pipe inputs to the radiant cooler. In addition, the temperature drop along the heat pipe is neglected, i.e., $T_p = T_1$.

Combining Eqs. (18) and (22)

$$\frac{A_p}{54\pi\left[\frac{T_M\epsilon\sigma}{\rho_s h_s}\right]^2\frac{\bar{\epsilon}}{\epsilon_p}T_E^4T_s^4} = \left[\frac{T_1}{T_s}\right]^4 - 2 + \frac{T_s}{T_1} - \frac{T_1^8}{T_1^4T_s^4} + 2\left[\frac{T_1}{T_E}\right]^4 - \left[\frac{T_s}{T_E}\right]^4 + \frac{K_3(T_E-T_1)/\sigma\epsilon_p T_1^4}{54\pi\left[\frac{T_M\bar{\epsilon}\sigma}{\rho_s h_s}\right]^2\left[\frac{\bar{\epsilon}}{\epsilon_p}\right]T_E^4T_s^4} \tag{23}$$

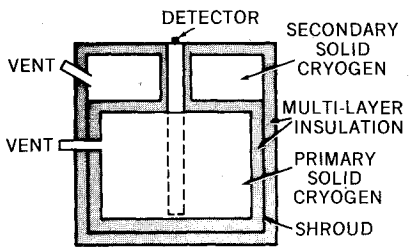

Fig. 7 Two stage solid cryogenic cooler.

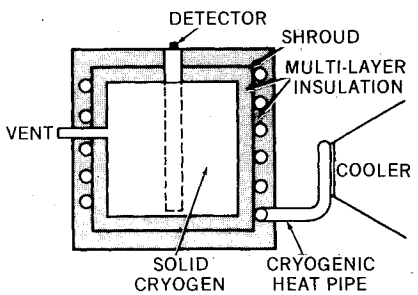

Fig. 8 Heat pipe/solid cryogen system.

Table 1 Comparison of secondary solid cryogen and radiant cooler/heat pipe weights ($T_1 = 160$ K)

Mission life (yr)	Secondary cryogen wt. ($\bar{\epsilon}=0.007$) (kg)	Radiant cooler/ heat pipe wt. (kg)
1	11	10
2	87	20

Equations (20) and (23) were used to estimate the weight of the secondary cryogen of a two stage cryogen system, and to compare it to the radiator and heat pipe weight of the hybrid system. Table 1 shows the results of these computations. Although the analysis presented here is a first cut at evaluating the hybrid cooler system, it appears from this table that for special applications the system offers substantial advantages over a two-stage solid cryogen cooler.

Conclusions

Heat pipes offer a number of practical advantages in cryogenic radiant cooler systems. However, the parasitic heat loads to the heat pipes require cooler sizes larger than presently used by NASA in the 80-100 K temperature range. An optimum heat pipe/radiant cooler will utilize heat pipes that are as small as practical consistent with satisfying transport requirements. The "1-*g*" test requirements will generally dictate the heat pipe's design. Projected transport requirements for heat pipes in cryogenic NASA coolers are approximately 3 W-m. This requirement along with the need to obtain meaningful "1-*g*" test results leads to composite wick designs. Axial grooves might also be used but they would have to be designed to provide 2-3 times more pumping in order to avoid "1-*g*" puddling and obtain good test results in the 80-100 K range.

Nitrogen and oxygen are the best fluids for operation over these temperatures. An analysis was made to determine their performance with an optimized composite slab geometry. The composite slab was selcted over an arterial design because it can provide more reliable priming. Results of the analysis indicate that a 1.27-cm o.d. pipe will be required to meet the 3 W-m transport with nitrogen. Although approximately 8 W-m can be obtained with this pipe at 80 K, its performance becomes marginal at 95 K. Oxygen, on the other hand, can provide an optimized performance of 30 W-m at 80 K which decreases to 14 W-m at 100 K with a 1.27-cm pipe. With the self-priming constraint imposed here, diameters of 1.0-cm or larger are required to satisfy the 3 W-m transport with oxygen and the composite slab design.

An analysis of a solid cryogen/heat pipe/radiant cooler system shows that, for special applications, a weight savings can be realized when compared to a two stage cryogenic system. More design analysis is warranted for this concept.

References

[1] Wright, J. and Pence, W., "Development of a Cryogenic Heat Pipe Radiator for a Detector Cooling System," ASME Paper No. 73-ENAs-47, July 1973.

[2] Brennan, P. et al., "Arterial and Grooved Cryogenic Heat Pipes," ASME Paper No. 71-WA/HT-42, Oct. 1971.

[3] Murray, D. and Foster, W., "A Cryogenic Heat Pipe for Satellite Sensor Cooling," ASME Paper No. 73-ENAs-50, July 1973.

[4] Kroliczek, E. and Brennan, P., "Axial Grooved Heat Pipes—Cryogenic Through Ambient," ASME Paper No. 73-ENAs-48, July 1973.

[5] Schlitt, K., Brennan, P., and Kirkpatrick, J., "Parametric Performance of Extruded Axial Grooved Heat Pipes from 80 to 300°K," *AIAA Progress in Astronautics and Aeronautics: Heat Transfer with Termal Control Applications*, Vol. 39, edited by M. Michael Yovanovich, MIT Press, Cambridge, Mass., 1975, pp. 215-234.

[6] Sherman, A. and Brennan, P., "Cryogenic and Low Temperature Heat Pipe/Cooler Studies for Spacecraft Application," AIAA Paper 74-753, Boston, Mass., 1974.

[7] *Heat Pipe Design Handbook*, DRD No. SE-345T, Aug. 1972, Dynatherm Corp.

[8] Kirkpatrick, J. and Brennan, P., "The Advanced Thermal Control Flight Experiment," *AIAA Progress in Astronautics and Aeronautics: Thermophysics and Spacecraft Thermal Control*, Vol. 35, edited by Robert G. Hering, MIT Press, Cambridge, Mass., 1974, pp. 409-430.